ISSN 1330-3651 (Print), ISSN 1848-6339 (Online)
https://doi.org/10.17559/TV-20220815140808
Original scientific paper

Optimal Design and Cogging Torque Minimization of a Permanent Magnet Motor for an Electric Vehicle

Hejra MSADDEK, Ali MANSOURI*, Hafedh TRABELSI

Abstract: With the increase of electric vehicle mobility, the integration of an electric motor inside the vehicle wheel is an interesting architecture for electric vehicles. This solution has the advantage of a great compactness of the motor and the elimination of mechanical transmission. This paper deals with the analytical modeling and the optimal dimension's finding of an in-wheel motor. An optimization procedure, based on Sequential Quadratic Programming SQP, is performed. The main objectives are the minimization of the machine weight and the maximization of its efficiency. While respecting constraints, an optimal machine with a weight of 11.61 kg and an efficiency of 93% is reached. To verify the satisfaction of the design requirements and the motor performances, finite element analysis (FEA), was applied. The comparison of induction results shows a good accuracy with a maximum error of 14%. The output torque and the air gap flux density are assessed. A maximum output torque of 90 Nm is achieved, and the slotting effect is noticed. Then the cogging torque of the machine is investigated; different rotor structures were studied. It is concluded, from results, that the topology with circular segmented magnets has the lowest cogging torque which does not exceed 7 Nm.

Keywords: analytical model; cogging torque; finite element analysis; optimization problem permanent magnet motor; SQP algorithm

1 INTRODUCTION

The pollution and the problem of greenhouse gases are two major problems that threaten the life of the human being. These problems are mainly due to the use of internal combustion engines. In addition, these engines make extensive use of fossil fuel resources. For this reason, the vehicle industries are encouraging researchers to overcome these problems by the emergence of electric vehicles [1-6]. Because of the cost of magnet materials and the complexity of the machine's structures, electric vehicles had not been very successful at the beginning [7]. With the technological progress of the last decade, the concept of electric cars has been again adopted. Great progress is being made in this domain [8-9]. In fact, an improvement in the electrical and magnetic performances of electric vehicles shows that these vehicles can substitute combustion vehicles [10-11]. The present work is situated in this context. We are looking to design an optimal permanent magnet motor for an electric traction application with a minimized cogging torque value.

A particular solution for electric vehicle design is adopted and studied, which is to independently drive every wheel by direct drive electric motor without any transmission or differential [12]. The motor is located inside the wheel. The weight of the motor is limited by the wheel dimensions. Therefore, the in-wheel motor design became a crucial optimization problem aiming to limit the motor weight without deteriorating other performances such as the motor efficiency. In the literature, few prototypes have been developed and many studies have been carried out in this context for electric and hybrid vehicle applications [13-17]. The comparison between different motors topologies done in [18] shows that permanent magnet machines are the best candidate for in wheel electric motor for electric vehicle application. Due to their numerous advantages, it has been mentioned in [19] that permanent magnet motors are widely applied for high performances applications.

Compared to other machines, it was shown in [20] that the machine with outer rotor presents numerous advantages: (i) the outer rotor machine is the most suitable for in-wheel vehicle applications, (ii) the large machine air gap diameter, enables the use of several poles, and (iii) the fact that the rotor is mounted on the outside makes the system more compact.

Depending on the shape of the induced electromotive force (*emf*) and their mode of feeding, permanent magnet machines can be classified into two families: 1) Permanent Magnet Synchronous Machines (PMSM) which are fed by sinusoidal currents and generally have sinusoidal *emf* and 2) Brushless Direct Current Motors (BDCM) which are fed by slot currents and generally have trapezoidal *emf*. The ease and the low cost of implementation as well as the simplicity of control of BDCM in comparison with PMSM [21] encouraged us to choose the BDCM for the present application. In [22], the design of a BLDC motor by means of FEA is proposed.

In this paper, the studied topology of the BDCM is described and the major geometric parameters are presented. An analytical model dealing with magnetic, electric, geometric, and thermal machine properties is presented. Then, for the design procedure of the considered machine according to the specifications, an optimization problem is formulated. In fact, this optimization problem is applied to minimize the motor weight and to maximize the efficiency. The optimization method is based on the Sequential Quadratic Programming (SQP). Once the optimization is done, a numerical modeling of the optimized topology, using the finite elements analysis, is defined. A comparison between analytical method and numerical ones is performed. The obtained results are discussed.

In the purpose of studying the machine performances, deep finite element analysis simulations were conducted. The air gap flux density and the output torque are investigated.

To minimize the cogging torque of the machine, the effect of the rotor structure studied. Therefore, the cogging torque is computed for different magnets shapes. In the literature, different techniques are used to minimize the cogging torque in permanent magnet motor [23-27]. In our work, we are interested in the method based on segmenting and spacing the magnets. According to the obtained results this technique has significantly reduced the cogging torque value.

2 MOTOR SIZING

2.1 Motor Geometry

As previously mentioned, the studied motor is a BDCM with trapezoidal *emf* fed by slots current. It has 36 slots, 24 poles with a surface mounted radial flux permanent magnet. Fig. 1 presents most of the geometrical parameters of the motor. Fig. 2 shows the geometry of the winding slots.

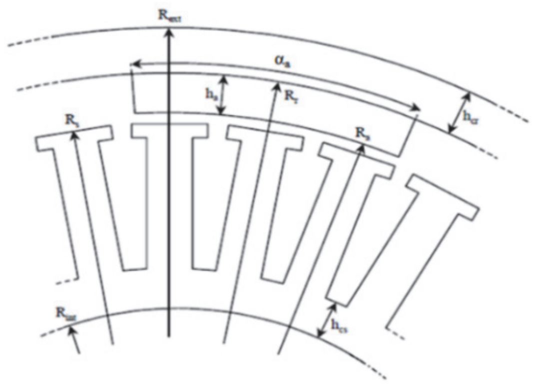

Figure 1 The geometrical dimensions of the motor

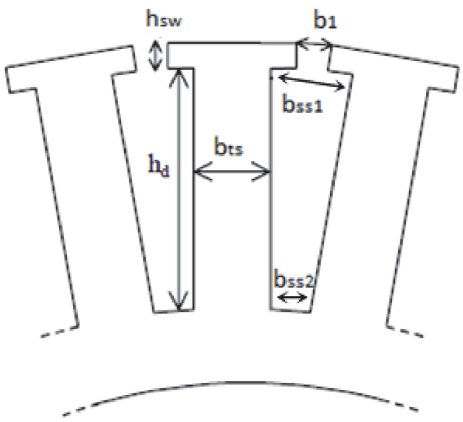

Figure 2 Slot dimensions

2.2 Machine Design

The most important step in the machine design is the definition of the characteristics to be achieved. Also, in the design procedure, many types of models are coupled to compute the motor parameters and to obtain the desired by the results. Tab. 1 illustrates the motor specifications.

Table 1 Motor specifications

Designation	Unit	Value
Nominal voltage	V	48
Outer rotor diameter	mm	262
Axial length	mm	73
Weight	kg	11
Efficiency	%	93

2.2.1 Electromagnetic Equations

In the design procedure, the number of coils is a crucial parameter.

This parameter is calculated by applying the Lenz law:

$$N = \frac{pE}{D_{exs} \cdot L_{machine} \cdot B_e \cdot 2\pi f} \tag{1}$$

where E is the *emf*, calculated from Lenz low.

$$E = N\frac{\mathrm{d}\varphi}{\mathrm{d}t} N\Omega \frac{\mathrm{d}\varphi}{\mathrm{d}\theta} \tag{2}$$

For a displacement of π/p with p as the number of pole pairs we have:

$$\frac{\mathrm{d}\varphi}{\mathrm{d}\theta} = \frac{2p\varphi}{\pi} \tag{3}$$

The expression of the *emf* is:

$$E = N\Omega\frac{2p\varphi}{\pi} \tag{4}$$

The flux expression is obtained by assuming a linear variation as function of the rotor position:

$$\varphi = B_e \cdot S_{pole} \tag{5}$$

The electromagnetic torque is:

$$C\Omega = 2EI \tag{6}$$

$$C = 2NIB_e\frac{S_e}{\pi} \tag{7}$$

2.2.2 Geometrical Equations

The major geometric parameters of the studied machine are illustrated in Fig. 1. These parameters make possible finding several relations. The rotor diameters are calculated as follows:

$$D_{inr} = D_{exs} + 2 \cdot \left(e + h_{pm}\right) \tag{8}$$

$$D_{exr} = D_{inr} + 2h_{cr} \tag{9}$$

The dimensions of the tooth dimensions shown in Fig. 2 are calculated as follows:

$$h_d = \frac{D_{exs}}{2} - \frac{D_{incs}}{2} - h_{sw} - h_{sy} \tag{10}$$

$$b_{ss1} = 2\frac{\pi}{N}\left[\frac{D_{exs}}{2} - h_{sw}\right] - b_{ts} \tag{11}$$

$$b_{ss2} = 2\frac{\pi}{N}\left[\frac{D_{incs}}{2} - h_{sy}\right] - b_{ts} \tag{12}$$

$$S_{enc} = \frac{h_{enc}\left(b_{ss1} + b_{ss2}\right)}{2} + b_1 + h_{sw} \tag{13}$$

2.2.3 Magnetic Equations

Some relations between geometric and magnetic equations are given by the flux conservation.

- Flux conservation between teeth and the airgap in the teeth's vicinity:

$$b_{ts} \cdot B_{ds} = \frac{D_{exs}}{2} \cdot \beta \cdot B_e \quad (14)$$

which allows calculating b_{ts} which is the width of the tooth.

- Flux conservation between magnet and rotor yoke:

$$B_{ry} \cdot h_{sy} \cdot K_{foi} = \frac{1}{2} B_a \cdot \alpha \cdot \left(e + \frac{D_{exs}}{2} \right) \quad (15)$$

- Flux conservation between the magnet and the air gap.

$$B_a \cdot \left(\frac{D_{exs}}{2} + e \right) \cdot \alpha \cdot k_{fui} = B_e \cdot \beta \cdot \frac{D_{exs}}{2} \quad (16)$$

where k_{fui} is the leakage factor ($k_{fui} < 1$) [15].

- Flux conservation between magnet and stator yoke

Identically, for the stator:

$$B_{sy} \cdot h_{sy} \cdot K_{foi} = \frac{1}{2} B_a \cdot \alpha \cdot \left(e + \frac{D_{exs}}{2} \right) \quad (17)$$

2.2.4 Thermal Equations

In the design procedure, it is very important to calculate the motor temperature which is described by Eq. (18). We suppose that the temperature is equal in different parts of the motor (magnet, rotor, stator, teeth) because we suppose that the convection thermal resistances are always more important than the thermal conduction resistances.

$$T = T_{ext} + \frac{P_j + P_{fer-s} + P_{fer-r} + P_m}{h_{conv} . S_{ext}} \quad (18)$$

where S_{ext} is the external surface of the motor.

$$S_{ext} = \frac{\pi}{2} D_{exr}^2 + \pi \cdot D_{exs} \cdot L_{machine} \quad (19)$$

2.2.5 Motor Weight and Efficiency

The motor's weight is computed from the sum of the weights of the different active parts: rotor, stator, magnet, and copper Eq. (20). The motor weight is the first objective to optimize. The second objective is the efficiency which is computed like in Eq. (21).

$$m_{mot} = m_{cr} + m_{cs} + m_{pm} + m_{copper} \quad (20)$$

$$\eta = \frac{C_{em} \cdot \Omega \cdot P_m}{C_{em} \cdot \Omega + P_j + P_{fer-r} + P_{fer-s}} \quad (21)$$

To calculate the copper losses, we must calculate the resistance per phase.

$$R_{ph} = \rho_{cuivre} \cdot \frac{L_{cuivre}}{S_{cuivre}} \quad (22)$$

hence the iron losses:

$$P_j = 2 \cdot R_{ph} \cdot I^2 \quad (23)$$

where ρ_{cuivre} is the resistivity of copper; L_{cuivre} is the length of the copper.

The iron losses in the rotor yoke P_{fer-r} and in the stator yoke P_{fer-s} are calculated as follows [28]:

$$P_{fer-r} = P_{specifique} \left(\frac{f}{f_{const}} \right)^{1,5} \cdot m_r \cdot \left(\frac{B_{ry}}{B_{const}} \right)^2 \quad (24)$$

$$P_{fer-s} = P_{specifique} \left(\frac{f}{f_{const}} \right)^{1,5} \cdot m_s \cdot \left(\frac{B_{sy}}{B_{const}} \right)^2 \quad (25)$$

3 OPTIMIZATION PROCEDURE

The machine geometry is completely defined through 9 parameters. To identify these unknown parameters, an optimization procedure must be done. In the literature several objective functions were used: minimization of the permanent magnet material weight, minimization of the total losses or maximization of the efficiency [20, 29, 30]. In our work, because the motor will be inside the wheel, the chosen objective function is the minimization of the motor weight. But we must not deteriorate the efficiency, so the second objective is the maximization of machine efficiency. An optimization design procedure is generally realized throughout three major steps. It begins by identifying the unknown machine design variables. Secondly the machine constraints and the objective function are defined and finally an appropriate solver is applied to find the optimum geometry satisfying all the requirements [31].

3.1 Optimization Variables

For the design, we have 9 optimization variables which are cited in the next table.

Table 2 Design variables

Variables	Unit	Designation
B_{ry}	T	Induction in the rotor yoke
B_{sy}	T	Induction in the stator yoke
B_{ds}	T	Induction in the teeth
B_e	T	Induction in the airgap
δ	mm	Thickness of the airgap
D_{exs}	mm	Outer diameter of the stator
D_{incs}	mm	Inner diameter of the stator
h_{pm}	mm	Thickness of the magnet
h_{sw}	mm	Slot wedge height

3.2 Constraints

Depending on the motor application, wheel-motor, many other constraints related to the wheel dimension have to be respected:
- The outer diameter of the rotor is fixed by the wheel diameter: D_{exr} = 262 mm.
- The axial length of the motor: $L_{machine}$ = 73 mm.

3.3 Specifications

According to the given specifications we have:
- The motor weight: approximately 11 kg.
- The efficiency: 93%

3.4 Optimization Problem

After selecting the objective functions, the optimization variables and the constraints, the optimization problem is expressed as follows:

$$\begin{cases} \min_X (m_{mot}) \\ \min_X (1-\eta) \\ under\ constraints \\ \begin{cases} 1 \le B_{ry} \le 1,7T \\ 1 \le B_{sy} \le 1,7T \\ 1 \le B_{ds} \le 1,7T \\ 0,85 \le B_\delta \le 0,95T \\ 0,8 \le \delta \le 2 \text{ mm} \\ 130 \le D_{incs} \le 200 \text{ mm} \\ 3 \le h_{pm} \le 5 \text{ mm} \\ 200 \le D_{exs} \le 250 \text{ mm} \\ D_{exr} = 262 \text{ mm} \end{cases} \end{cases} \quad (26)$$

4 RESULTS

At first the optimization problem is solved by means of the SQP algorithm. The variations of the two objective functions, weight and efficiency, are illustrated in Fig. 3 and 4. According to these figures, we can clearly notice that after 140 iterations the objectives tend towards specifications.

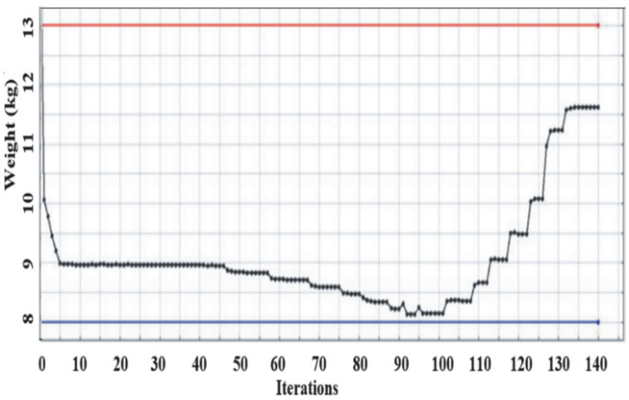

Figure 3 Weight variation according to iterations

Fig. 5 shows the variation of the weight of the motor according to its efficiency. From this figure, two regions can be distinguished. The first region is located on the left of the point 1 in which the motor is unfeasible. In fact, we notice that in this region the weight of the engine decreases while the efficiency increases which is not logical, because if the weight decreases, then the weight of all the materials decreases and as a result the efficiency decreases. So, the second region of the curve, in which the motor is feasible, is located on the right of the point 1.

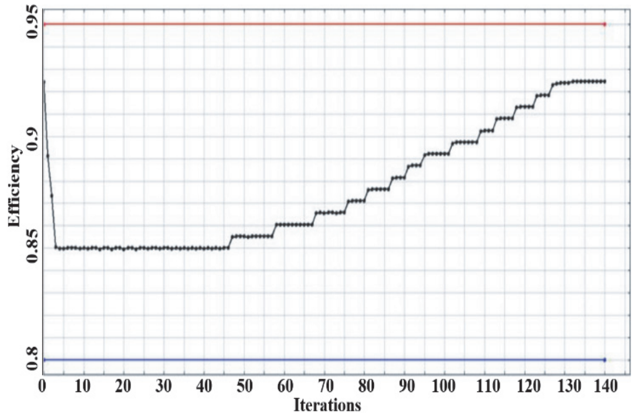

Figure 4 Efficiency variation according to iterations

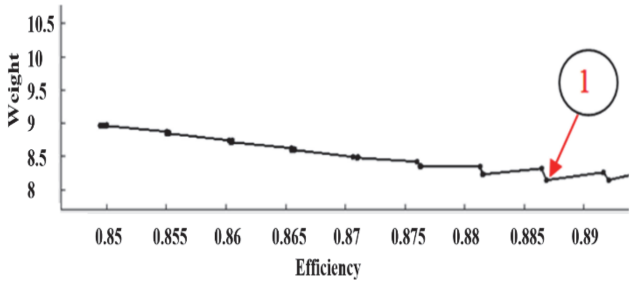

Figure 5 Front of Pareto for weight and efficiency

The final point of the optimization is meeting the specification (weight = 11.61 Kg, efficiency = 92.24% which is close to 93%). The outer diameter constraint of the rotor is respected (D_{exr} = 262 mm) with an active length of the machine $L_{machine}$ = 73 mm.

The different machine regions weights are illustrated in Tab. 3.

Table 3 Weight of different parts of the motor

Entities	Before optimization	After optimization
Copper weight / kg	1,15	0,45
Rotor weight / kg	3,03	3,67
Stator weight / kg	9,48	6,35

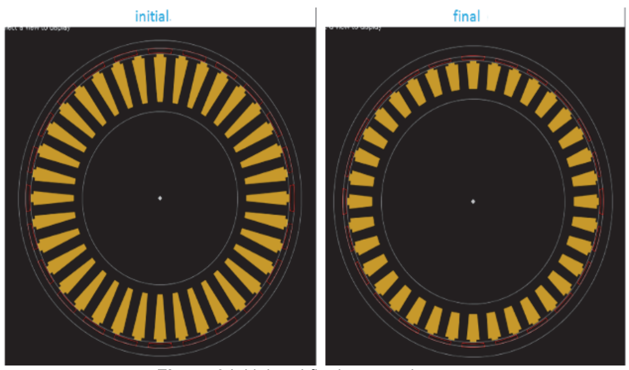

Figure 6 Initial and final geometries

Fig. 6 presents the geometry of the motor before and after optimization.

The obtained design variables, subject of the optimization, are presented in tab. 4.

Table 4 Motor geometric parameters

Variables	Initial value	Final value
b_1 / mm	7	6
b_d / mm	14	13
b_{ts} / mm	1,4	1,7
B_e / T	8,8	7,7
b_{ss1} / mm	12,5	12,6
b_{ss2} / mm	5,6	8,8
D_{exr} / mm	273	262
h_{ry} / mm	6,8	8,6
h_{sy} / mm	8,1	8,6

5 VERIFICATION WITH FINITE ELEMENT ANALYSIS

At performing our optimization procedure, we have obtained the optimal geometric dimensions of the motor. Then, these parameters will be used to model the machine by means of the finite element software. This step is carried out to validate the obtained optimization results. FEA is a powerful tool used by reserchers to analyse electromagnetic devices [32-33]. In our work, the magnetic field problems solution is obtained using the magnetic vector potential (A).

For reasons of periodicity and symmetry in the machine [34], the study is limited to 2-D and to 1/12 of the machine. To assure the FEA model continuity, additional boundary conditions are applied. A particular attention is paid to the meshing method to ensure the rotor movement. Indeed, a sliding line is constructed in the middle of the air gap and periodicity boundary contidions were applied.

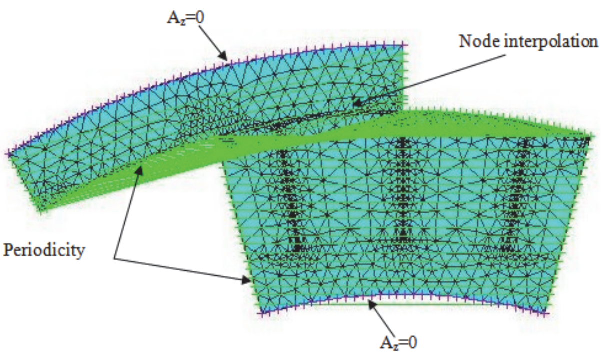

Figure 7 Study domain and boundary conditions

The previous figure (Fig. 7) illustrates the study domain of the ivestigated machine in which are reported the boundary conditions.

The magnetic flux densities through the magnetic circuit are summarized in Tab. 5.

Table 5 Weight of different parts of the motor

	B_{ry}	B_{sy}	B_δ
Analytical value / T	1,5	1,5	0,9
Numerical value / T	1,63	1,66	1,05
Error / %	8	9	14

Referring to tab. 5, we note that the difference between the FEA results and the analytical values is slight, which validates our optimization procedure.

While considering the optimum machine parameters, the air gap flux density and the output torque versus the rotor position are computed. The obtained results are respectively illustrated in Fig. 8 and Fig. 9.

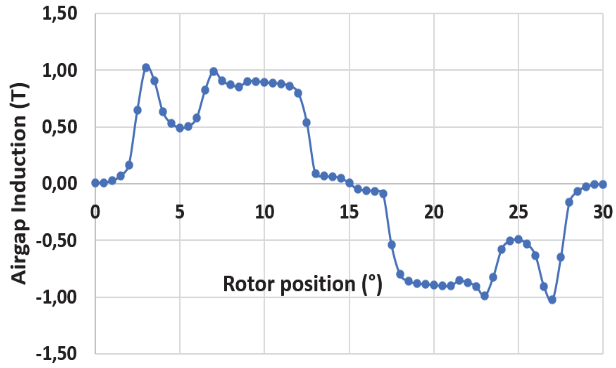

Figure 8 Airgap flux density variations

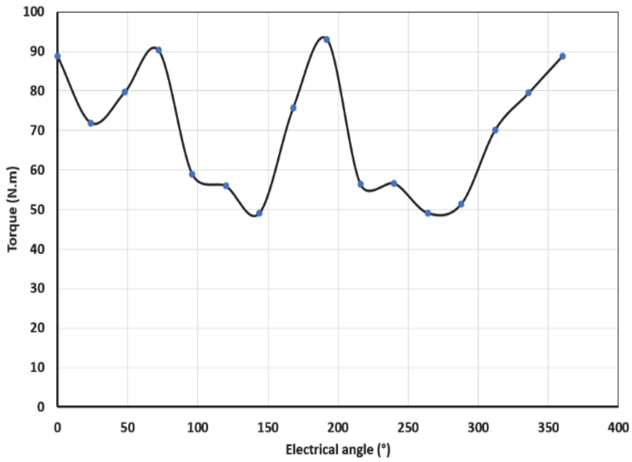

Figure 9 Airgap Output torque

According to these previous figures, we can clearly notice that the airgap flux density waveform turns to be trapezoidal, the slotting effect is also remarkable. Concerning the output torque, we can notice that a maximum value of 90 Nm is reached, and a high ripple torque is also detected. This torque can induce vibration and noise in the permanent magnet hub. Therfore, it must be considered when developping the motor control strategy.

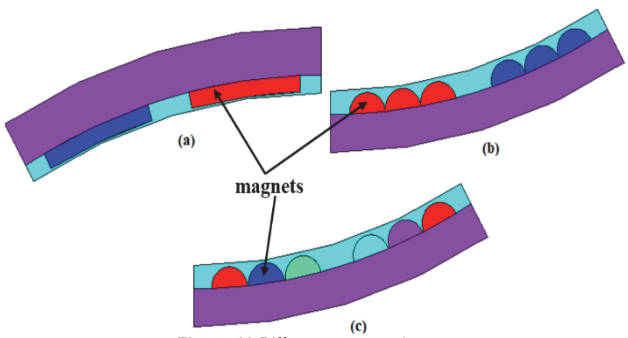

Figure 10 Different magnet shapes

In a brushless permanent magnet machine, cogging torque is due to the magnetic attraction between the permanent magnets mounted in the rotor and the stator teeth. In this section, the effect of different permanent magnets shapes: conventional magnets (a), segmented circular magnets (b) and segmented circular spaced magnets (c) on the cogging toque is studied. The obtained results are illustrated in Fig. 10.

According to these results, we can clearly notice that:

- The machine with circular permanents magnets presents the highest cogging torque reaching a maximum value equal to 35 Nm.
- The topology with circular segmented magnets has the lowest value of the cogging torque which does not exceed 7 Nm. Therefore, a decrease of about 28 Nm is obtained compared to the first machine.

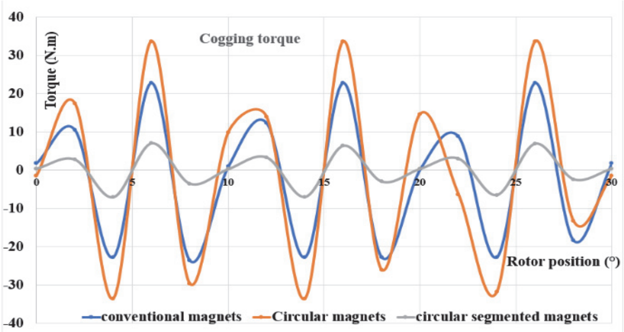

Figure 11 Study domain and boundary conditions

6 CONCLUSION

In this work, an analytical model, required to optimize a brushless direct current machine, has been developed. This motor will be used for the application of in-wheel motor electric vehicle. This application makes many constraints for motor design. In order to find optimal motor geometry, an optimization procedure, based on Sequential Quadratic Programming (SQP) has been presented. The purpose of this optimization is the minimisation of motor weight and the maximization of its efficiency.

To achieve this goal, many simulations have been carried out to find the optimum machine design variables. Finally, the optimization is finished, and optimal motor parameters are given. The comparison of the obtained results with those based on FEA, shows the effectiveness of the proposed optimization procedure. An investigation of the machine performances, by means of FEA, is carried out. The existence of a high ripple torque and cogging toque was shown. To minimize the machine cogging torque, deep FEA was carried out. Different machine rotor structures were investigated. A decrease of the cogging torque value of about 80% is achieved.

Despite the considerable improvement of the machine performances, several other works remain essential such as the analytical model improvements, the investigation of different stator and rotor structures and the developpement of the appropriate control strategy of the studied motor.

7 REFERENCES

[1] Amakrishnan, K., Gobbi, M., & Mastinu, G. (2015). Multi-Objective Optimization of In-Wheel Motor Powertrain and Validation Using Vehicle Simulator. *10th Int. Conf. on Eco. Veh. and Ren. Ene.*, Monte Carlo, Monaco, 1-9. https://doi.org/10.1109/EVER.2015.7112919

[2] Liu, M., Gu, F., & Zhang, Y. (2017). Ride Comfort Optimization of In-Wheel-Motor Electric Vehicles with In-Wheel Vibration Absorbers. *Energies*, *10*(10). https://doi.org/10.3390/en10101647

[3] Xiaoyuan, W., Sijia, X., Chunpeng, L., & Xiang, L. (2017). Field-Weakening Performance Improvement of the Yokeless and Segmented Armature Axial Flux Motor for Electric Vehicles. *Energies*, *10*(10). https://doi.org/10.3390/en10101492

[4] Stefan, B., Marius, D., Mihai, C., Alexandru, M. P., Petre, D. T., & Claudiu, A. O. (2022). Experimental Tests on a Spoke-Type Permanent Magnets Synchronous Machine for Light Electric Vehicle Application. *App. Sci.*, *12*(6). https://doi.org/10.3390/app12063019

[5] Hoyun, W., Yang, K. H., Minyeong, C., Jonathan, P., Briana, B., Seungdeog, C., Shuhui, L., Hwan, S. Y., Timothy, A. H., Jongkook, L., & Tae, W. L. (2022). Novel Design of Six-Phase Spoke-Type Ferrite Permanent Magnet Motor for Electric Truck Application. *Energies*, *15*(6). https://doi.org/10.3390/en15061997

[6] Hoyun, W., Yang, H. K., Woncheo, L., Minyeong, C., Shuhui, L., & Hwan, S. Y. (2019). Low Torque Ripple Spoke-Type Permanent Magnet Motor for Electric Vehicle. *IEEE Int. Elec. Mach. & Drives Conf.*, San Deigo, USA, 945-950.

[7] Gillon, F. (2009). *Méthodologie de conception optimale des composants électromagnétiques*. Central school of Lille.

[8] Hwang, C., Li, P., & Liu, C. (2012). Optimal design of permanent magnet linear synchronous motor with low cogging force. *IEEE Tran. on mag.*, *48*(2), 1039-1042. https://doi.org/10.1109/TMAG.2011.2172578

[9] Engin, H., Mustafa, C. A., & Uğur, D. (2015). A new approach in application and design of toroidal axial-flux permanent magnet open-slotted NN type (TAFPMOS-NN) motor. *Tehnički Vjesnik*, *22*(5), 1193-1198. https://doi.org/10.17559/TV-20140704100736

[10] Mi, C. C. (2006). Analytical design of permanent magnet traction drive motor. *IEEE Tran. on Magn.*, *42*(7), 1861-1866. https://doi.org/10.1109/TMAG.2006.874511

[11] Chen, G. H. (1996). Design of a permanent-magnet direct-driven wheel motor drive for electric vehicle. *27th Ann. IEEE Pow. Elec. Spe. Con.,* 1933-1939. https://doi.org/10.1109/PESC.1996.548845

[12] Shrivastava, N. & Brahmin, A. (2014). Design of 3-Phase BLDC Motor for Electric Vehicle Application by Using Finite Element Simulation. *Int. J. of Eme. Tech. and Adv. Eng.*, *4*(1), 140-145.

[13] Msaddek, H., Mansouri, A., & Trabelsi, H. (2015). Optimization of In-Wheel Permanent Magnet Synchronous for electric car. *Int. J. of Ene. Opt. and Eng.*, *4*(3), 1-17. https://doi.org/10.4018/IJEOE.2015070101

[14] Brisset, S. & Brochet, P. (2005). Analytical model for the optimal design of a brushless DC wheel motor. *COMPEL*, *24*(3), 829-848. https://doi.org/10.1108/03321640510612952

[15] Tuncay, R. N., Ustun, O., & Yilmaz, M. (2011). Design and implementation of an electric drive system for in-wheel motor electric vehicle applications. *2011 IEEE Veh. Pow. and Pro. Conf., Chicago, Illinois, USA.* https://doi.org/10.1109/VPPC.2011.6043070

[16] Cakir, K. & Sabanovic, A. (2006). In-wheel motor design for electric vehicles. *9th IEEE Int. Work. on Adv. Mot. Con.*, 613-618. Istanbul, Turkey. https://doi.org/10.1109/AMC.2006.1631730

[17] Mansouri, A. (2016). Conception et optimisation multi-objectifs d'un moteur à aimants permanents destiné pour un véhicule électrique. *HDR, Université de Gafsa, Tunisie, 2016.*

[18] Boussad, B. (2012). *Contribution à la modélisation des systèmes couples machines convertisseurs : application aux machines a aimants permanents*. PHD thesis, université de Mouloud Mammeri, Algérie.

[19] Uğur, D. & Mustafa, C. A. (2017). Using Taguchi method in defining critical rotor pole data of LSPMSM considering the

power factor and efficiency. *Tehnički Vjesnik*, *24*(2), 347-353. https://doi.org/10.17559/TV-20140714225453
[20] Zaaraoui, L. & Mansouri, A. (2021). Optimization and finite element analysis of an in-wheel permanent magnet motor. *Mal. J. of Fun. and App. Sci.*, *17*(1), 104-108. https://doi.org/10.11113/mjfas.v17n1.1981
[21] Kim, D., Shin, K., Kim, Y. & Choen, J. (2010). Integrated design of in-wheel motor system on rear wheels for small electric motor. *World Electr. Veh. J.*, *4*(3), 597-60. https://doi.org/10.3390/wevj4030597
[22] Mustafa, D. & Ali, F. B. (2015). The analysis of different techniques for speed control of permanent magnet synchronous motor. *Tehnički Vjesnik*, *22*(4), 947-952. https://doi.org/10.17559/TV-20140912141639
[23] Yong, Y. & Xudong, W. (2022). Method of Cogging Torque Reduction for Built-in Permanent Magnet Synchronous Motor. *J. of Phy. Conf. Ser., 8th Int. Sym. on Sen., Mech. and Aut. Sys., Suzhou, China*, 1-5. https://doi:10.1088/1742-6596/2170/1/012046
[24] Yongda, S., Zhaoyu, Z., Siyang, Y., Fengge, Z., & Yuan, Z. (2021). Analysis and reduction of cogging torque in direct-drive external-rotor permanent magnet synchronous motor for belt conveyor application. *IET Elec. Pow. App., 15*(6), 668-680. https://doi.org/10.1049/elp2.12048
[25] Andrzej, B., Tomasz, D., Dawid, K., & Tomasz, K. (2022). Reduction in the Cogging Torques in the DCEFSM Motor by Changing the Geometry of the Rotor Teeth. *Energies*, *15*(7). https://doi.org/10.3390/en15072455
[26] Mehdi, A. & Hamed, K. (2018). Cogging torque reduction of Interior Permanent Magnet Synchronous Motor (IPMSM). *Sci. Iran.*, *25*(3), 1471-1477. https://doi.org/10.24200/sci.2017.4365
[27] Handran, P., Mylsamy, K., & Umapathy, P. (2022). Conceptual Design and Material Analysis of BLDC Motor Using FEA Tools for Electric Vehicle Applications. *Tehnički Vjesnik*, *29*(3), 1010-1018. https://doi.org/10.17559/TV-20210425201219
[28] Msaddek, H. (2017). *Modélisation, conception et optimisation des moteurs électriques pour l'application des véhicules électriques à moteurs-roues*. PhD thesis, National School of Engineering of Gabes, Tunisia.
[29] Zaaraoui, L., Mansouri, A., & Smairi, N. (2022). Nmopso: an improved multiobjective PSO algorithm for permanent magnet motor design. *U.P.B. Sci. Bull., Ser. C*, *84*(1), 201-214.
[30] Zaaraoui, L., Mansouri, A., & Smairi, N. (2022). Design and Optimization of an In-wheel Unequal Stator Teeth Motor". *Int. J. of Ren. Ener. Res.*, *12*(1), 284-293. https://doi.org/10.20508/ijrer.v12i1.12723.g8397
[31] Msaddek, H., Mansouri, A., & Trabelsi, H. (2014). Optimal design of a permanent magnet synchronous motor: application of in-wheel motor. *5th Int. Ren. Ene. Cong., Hammamet, Tunisia.* https://doi.org/10.1109/IREC.2014.6826903
[32] Zheng, L., Ruodong, Z., & Qunjing, W. (2017). Electromagnetic system analysis and improvement of a novel 3-dof deflection type permanent magnet motor. *Tehnički Vjesnik*, *24(2),* 249-256. https://doi.org/10.17559/TV-20140110064840
[33] Asim, G. Y. & Mustafa, T. (2017). Efficiency improvement in induction motor by slitted tooth core design. *Tehnički Vjesnik*, *24*(5), 1291-1296. https://doi.org/10.17559/TV-20140325133232
[34] Msaddek, H., Mansouri, A., & Trabelsi, H. (2014). On the dynamic modelling of inset permanent magnet motor. *11th Int. multi-conf. on Sys. Sig. & Dev., Barcelona, Spain.* https://doi.org/10.1109/SSD.2014.6808836

NOMENCLATURE

B_a - Maximum airgap flux density above the magnets. b_{ts} - Stator tooth width. b_{ss1} - Outer stator slot width. b_{ss2} - Inner stator slot width. B_{ds} - Stator teeth flux density. B_{sy} - Stator yoke flux density. B_{ry} - Rotor yoke flux density. B_e - Fundamental air gap flux density. b_1 - Slot opening. C - Electromagnetic torque. D_{exs} - Stator outer diameter. D_{exr} - Rotor outer diameter. D_{incs} - Rotor inner diameter. D_{incr} - Stator inner diameter. δ - Airgap. E - Electromotive force. f - Frequency. h_{conv} - Coefficient of conviction. h_{pm} - Magnet thickness. h_{sy} - Stator yoke height. h_{sw} - Slot wedge height.	I - Rated current loading. K_{foi} - Coefficient of expansion. k_{fui} - Leakage coefficient- $L_{machine}$ - Active machine axial length. m - Number of phases. m_{mot} - Motor weight. m_{cr} - Weight of rotor yoke. m_s - Weight of the stator. m_{copper} - Weight of copper. m_{pm} - Weight of the magnet. N - Number of coil. p - Pair pole number. P_{em} - Electromagnetic power. P_j - Copper losses. $P_{f\text{-}s}$ - Stator iron losses. $P_{f\text{-}r}$ - Rotor iron losses. P_m - Mechanical losses. T - Magnet temperature. Ω - Rated speed- η - Efficiency. A - Opening angle of the pole. B - Opening angle of the teeth.

Contact information:

Hejra MSADDEK, PdD
CES Laboratory, Engineering School of Sfax,
3038, Sfax, Tunisia
E-mail: msaddek_hejra@yahoo.fr

Ali MANSOURI, Associate Professor
(Corresponding author)
University of Gafsa,
Higher Institute of Applied Sciences and technology,
TEMI Lab 2100, Gafsa, Tunisia
E-mail: ali.mansouri@isetgf.rnu.tn

Hafedh TRABELSI, Professor
CES Laboratory, Engineering School of Sfax,
3038, Sfax, Tunisia
E-mail: hafedh.trabelsi@enis.tn